The Slipping Approach to Self-Assembling [*n*]Rotaxanes†

Masumi Asakawa,‡ Peter R. Ashton,‡ Roberto Ballardini,§ Vincenzo Balzani,⊥ Martin Bělohradský,‡ Maria Teresa Gandolfi,⊥ Oldrich Kocian,‡ Luca Prodi,⊥ Françisco M. Raymo,‡ J. Fraser Stoddart,*,‡ and Margherita Venturi⊥

Contribution from The School of Chemistry, The University of Birmingham, Edgbaston, Birmingham B15 2TT, UK, Istituto FRAE-CNR, via Gobetti 101, I-40129 Bologna, Italy, and Dipartimento di Chimica "G. Ciamician" dell'Università, via Selmi 2, I-40126 Bologna, Italy

Received May 30, 1996. Revised Manuscript Received October 29, 1996⊗

Abstract: A synthetic approach—namely slippage—to self-assembling [*n*]rotaxanes incorporating π-electron deficient bipyridinium-based dumbbell-shaped components and π-electron-rich hydroquinone- and/or dioxynaphthalene-based macrocyclic polyether components has been developed. The kinetics of rotaxane formation by the slipping procedure were investigated by absorption UV−visible and ^{1}H-NMR spectroscopies in a range of temperatures and solvents, varying systematically the size of both the stoppers and the macrocyclic components. As expected, the rate constants for these processes are affected by the size complementarity between macrocycles and stoppers. Furthermore, the enthalpic and entropic contributions to the free energies of activation associated with the slippage and the effect of solvent polarity upon the outcome of these processes have been evaluated. In addition, the spectroscopic and electrochemical properties of some of the rotaxanes are presented and discussed with reference to the properties of their chromophoric and electroactive units.

Introduction

The slippage approach to self-assembling[1] rotaxanes[2] is illustrated schematically in Figure 1. The macrocycle **M** and the dumbbell-shaped compound **D** are formed separately and then mixed in solution. In order to self-assemble the rotaxane **R**, slipping-on of the macrocycle **M** over the stoppers of **D** is required. As a result, the energy barrier $\Delta G^{\ddagger}_{on}$ has to be overcome. Thus, heating of the solution at an appropriate temperature *T* is required. An equilibrium between the newly formed rotaxane **R** and the *free* components **M** and **D** is therefore achieved at *T*. By contrast, the noncovalent bonding interactions existing between the dumbbell-shaped and macrocyclic components within the rotaxane **R** make the energy barrier $\Delta G^{\ddagger}_{off}$ of the slipping-off process higher than that of the slipping-on pushing the equilibrium toward **R** [$\Delta G^{\ddagger}_{off} > \Delta G^{\ddagger}_{on}$; the difference between these two values corresponds to the binding energy $\Delta G°$ ($\Delta G^{\ddagger}_{off} - \Delta G^{\ddagger}_{on} = \Delta G°$)]. On cooling the solution down, the energy barrier for both slipping-on and slipping-off processes cannot be overcome, *i.e.* ideally, no interconversion occurs between the rotaxane **R** and *free* components **M** and **D** and *vice versa*. As a result, **R** becomes kinetically stable and its separation from **M** and **D** can be achieved employing the usual chromatographic techniques.

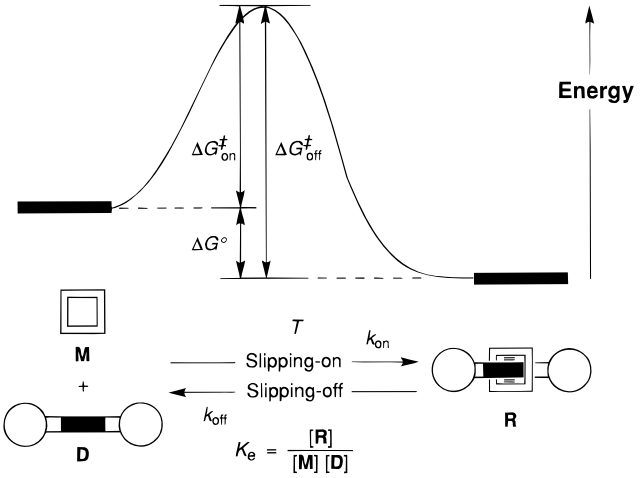

Figure 1. Schematic illustration of the slipping approach to rotaxanes.

In previous research,[3] we have demonstrated the efficiency of the slipping approach by self-assembling a number of linear and branched [2]rotaxanes, [3]rotaxanes, and [4]rotaxanes incorporating π-electron rich hydroquinone-based macrocyclic polyethers and π-electron deficient bipyridinium-based dumbbell-shaped components. In particular, the dumbbell-shaped compounds **H-D**, **Me-D**, **Et-D**, and ***i*-Pr-D** (Scheme 1), incorporating one bipyridinium recognition site and bis(4-*tert*-butylphenyl)-4-R-phenylmethane-based stoppers in which the size of the R groups was varied systematically, were synthesized.[3a,e] Heating MeCN solutions of each dumbbell-

† Molecular Meccano, Part 12. For Part 11, see: Asakawa, M.; Ashton, P. R.; Boyd, S. E.; Brown, C. L.; Gillard, R. E.; Kocian, O.; Raymo, F. M.; Stoddart, J. F.; Tolley, M. S.; White, A. J. P.; Williams, D. J. *J. Org. Chem.* In press.

‡ University of Birmingham.

§ FRAE-CNR.

⊥ University of Bologna.

⊗ Abstract published in *Advance ACS Abstracts,* December 15, 1996.

(1) (a) Whitesides, G. M.; Simanek, E. R.; Mathias, J. P.; Seto, C. T.; Chin, D. N.; Mammen, M.; Gordon, D. M. *Acc. Chem. Res.* **1995**, *28*, 37−44. (b) Lawrence, D. S.; Jiang, T.; Levett, M. *Chem. Rev.* **1995**, *95*, 2229−2260. (c) Raymo, F. M.; Stoddart, J. F. *Curr. Op. Coll. Interf. Sci.* **1996**, *1*, 116−126. (d) Philp, D.; Stoddart, J. F. *Angew. Chem., Int. Ed. Engl.* **1996**, *35*, 1154−1196.

(2) (a) Gibson, H. W.; Bheda, M. C.; Engen, P. T. *Prog. Polym. Sci.* **1994**, *19*, 843−945. (b) Amabilino, D. B.; Stoddart, J. F. *Chem. Rev.* **1995**, *95*, 2725−2828. (c) Bělohradský, M.; Raymo, F. M.; Stoddart, J. F. *Collect. Czech. Chem. Commun.* **1996**, *61*, 1−43.

(3) (a) Ashton, P. R.; Bělohradský, M.; Philp, D.; Stoddart, J. F. *J. Chem. Soc., Chem. Commun.* **1993**, 1269−1274. (b) Ashton, P. R.; Bělohradský, M.; Philp, D.; Spencer, N.; Stoddart, J. F. *J. Chem. Soc., Chem. Commun.* **1993**, 1274−1277. (c) Amabilino, D. B.; Ashton, P. R.; Bělohradský, M.; Raymo, F. M.; Stoddart, J. F. *J. Chem. Soc., Chem. Commun.* **1995**, 751−753. (d) Bělohradský, M.; Philp, D.; Raymo, F. M.; Stoddart, J. F. In *Organic Reactivity: Physical and Biological Aspects*; Golding, B. T., Griffin, R. J., Maskill, H., Eds.; RSC Special Publication No. 148: Cambridge, 1995; pp 387−398. (e) Ashton, P. R.; Ballardini, R.; Balzani, V.; Bělohradský, M.; Gandolfi, M. T.; Philp, D.; Prodi, L.; Raymo, F. M.; Reddington, M. V.; Spencer, N.; Stoddart, J. F.; Venturi, M.; Williams, D. J. *J. Am. Chem. Soc.* **1996**, *118*, 4931−4951.

S0002-7863(96)01817-3 CCC: $14.00

Scheme 1

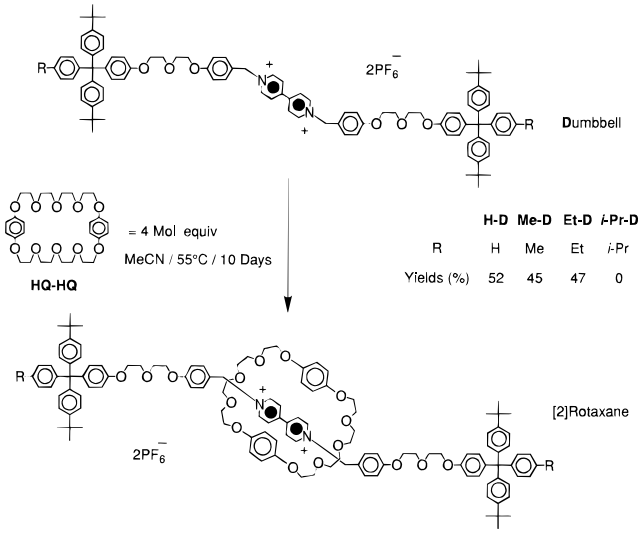

Scheme 2

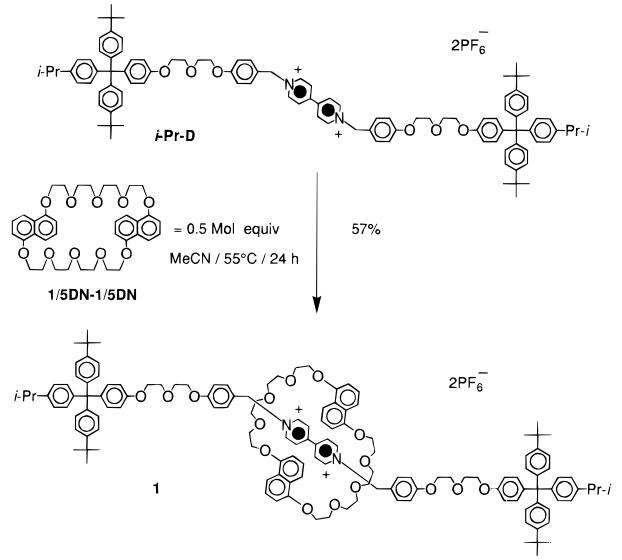

shaped compound at 55 °C with 4 molar equiv of the hydroquinone-based macrocycle **HQ-HQ** affords[3a,e] the corresponding [2]rotaxanes in good yields when R is equal to H, Me, and Et: no rotaxane, however, is isolated when R is equal to *i*-Pr. Thus, the energy barrier $\Delta G^{\ddagger}_{on}$ for the slipping-on of **HQ-HQ** becomes insurmountable at 55 °C on going from Et to *i*-Pr substitution. In the wake of these results, we decided to investigate, in some detail, the kinetics of the slipping approach to rotaxanes by varying systematically the size of both macrocyclic (compound) component and the stoppers at the ends of the dumbbell-shaped (compound) component. We report here the results of these kinetic studies, as well as the syntheses, spectroscopic, and electrochemical properties of rotaxanes incorporating bipyridinium-based dumbbell-shaped components and hydroquinone-based and/or dioxynaphthalene-based macrocyclic polyether components.

Results and Discussion

Synthesis.[4] The energy barrier $\Delta G^{\ddagger}_{on}$ associated with the slipping-on (Scheme 1) of the hydroquinone-based macrocyclic polyether **HQ-HQ** over the stoppers of the dumbbell-shaped compound ***i*-Pr-D** is high at 55 °C—*i.e.* the "*i*-Pr-substituted" stoppers are too bulky for the *small* hydroquinone-based macrocycle. Thus, passage of **HQ-HQ** over the bis(4-*tert*-butylphenyl)-4-isopropylphenylmethane-based stoppers is not possible at this temperature and the corresponding [2]rotaxane is not formed. However, we reasoned that, since replacement of both of the hydroquinone rings incorporated within the macrocyclic polyether by 1,5-dioxynaphthalene units enlarges the size of the cavity of the macrocycle, the energy barrier $\Delta G^{\ddagger}_{on}$ should be lowered. Indeed, on heating (Scheme 2) a MeCN solution of the 1,5-dioxynaphthalene-based macrocycle **1/5DN-1/5DN** and the dumbbell-shaped compound ***i*-Pr-D** at 55 °C during 24 h, the [2]rotaxane **1** self-assembles[5] in a yield of 57%. Hence, although the "*i*-Pr-substituted" stoppers are bulky enough to prevent the slipping-on of the hydroquinone-based macrocycle **HQ-HQ**, the passage over them of the larger 1,5-dioxynaphthalene-based macrocycle **1/5DN-1/5DN** can occur under otherwise identical conditions. Furthermore, the slipping-on (Scheme 1) of **HQ-HQ** over the stoppers of the dumbbell-shaped components **H-D**, **Me-D**, and **Et-D** requires *ca.* 10 days for completion and the yields of the corresponding [2]rotaxanes are 52, 45, and 47%, respectively. On the contrary, the self-assembly of the [2]rotaxane **1**, incorporating **1/5DN-1/5DN** as the macrocyclic component, is achieved in a yield of 57% after only 1 day.

The "*i*-Pr-substituted" stoppers are too bulky for the slipping-on of the **HQ-HQ** macrocycle—*i.e.* $\Delta G^{\ddagger}_{on}$ and, as a result, $\Delta G^{\ddagger}_{off}$ are too high. However, these stoppers can be employed to self-assemble rotaxanes, incorporating **HQ-HQ** as the macrocyclic component, by employing the threading methodology.[3e] Reaction (Scheme 3) of the bis(hexafluorophosphate) salt **[BPYPYXY][PF$_6$]$_2$** with the stoppers ***i*-Pr-S** in the presence of only 1.1 molar equiv of **HQ-HQ** affords[5] the [2]rotaxane **2** in a yield of 19%, after counterion exchange. As a result of the size of the "*i*-Pr-substituted" stoppers incorporated within the [2]rotaxane **2**, neither the slipping-on ($\Delta G^{\ddagger}_{on}$ too high) of a second macrocyclic **HQ-HQ** component nor the slipping-off ($\Delta G^{\ddagger}_{off}$ too high) of the **HQ-HQ** macrocyclic component already *trapped* on the dumbbell-shaped component of **2** can be achieved under the usual conditions employed to induce slipping—namely, 55 °C at ambient pressure. Thus, a 1,5-dioxynaphthalene-based **1/5DN-1/5DN** macrocycle can be slipped-on over the stoppers of **2**, leaving, in place on the dumbbell-shaped component, the **HQ-HQ** macrocycle already incorporated within the [2]rotaxane **2** by employing the usual slippage conditions. By heating (Scheme 3) a MeCN solution of the [2]rotaxane **2** in the presence of 3 molar equiv of the **1/5DN-1/5DN** macrocycle at 55 °C during 48 h, the [3]rotaxane **3** incorporating two constitutionally different macrocyclic components is self-assembled[5] in a yield of 49%.

^{1}H-NMR Spectroscopy. The chemical shifts (δ) for the protons in the α- and β-positions with respect to the nitrogen

(4) The compounds bis[4-(4-pyridyl)pyridinium]-*p*-xylene bis(hexafluorophosphate) and 4,4′-dimethylbipyridinium bis(hexafluorophosphate)—commonly known as paraquat—are abbreviated to **[BPYPYXY][PF$_6$]$_2$** (Scheme 3) and **[PQT][PF$_6$]$_2$** (Figure 2), respectively. The compounds methoxybenzene, 1,4-dimethoxybenzene, 1,5-dimethoxynaphthalene, and 2,7-dimethoxynaphthalene are abbreviated to **MB**, **1/4DMB**, **1/5DMN**, and **2/7DMN** (**Figures 4** and **5**), respectively. The acronyms employed to indicate the dumbbell-shaped compounds depicted in Scheme 1 and Figure 3 are composed of the common alphabetical notation corresponding to the R groups attached to the stoppers followed by the letter **D** which stands for dumbbell. The bis(*tert*-butylphenyl)-4-isopropylphenylmethane-based chloride shown in Scheme 3 and the tetraarylmethane-based model compound shown in Figure 5 are abbreviated to ***i*-Pr-S** and **R-S** where **S** stands for stopper. The acronyms, corresponding to the macrocyclic polyethers depicted in Figure 2, indicate the nature of the two aromatic units incorporated into each macrocycle. Thus, **HQ**, **1/5DN**, and **2/7DN** stand for hydroquinone, 1,5-dioxynaphthalene, 2,7-dioxynaphthalene, and so on. Numbers are employed for the remaining compounds.

(5) Amabilino, D. B.; Ashton, P. R.; Bělohradský, M.; Raymo, F. M.; Stoddart, J. F. *J. Chem. Soc., Chem. Commun.* **1995**, 747−750.

Scheme 3

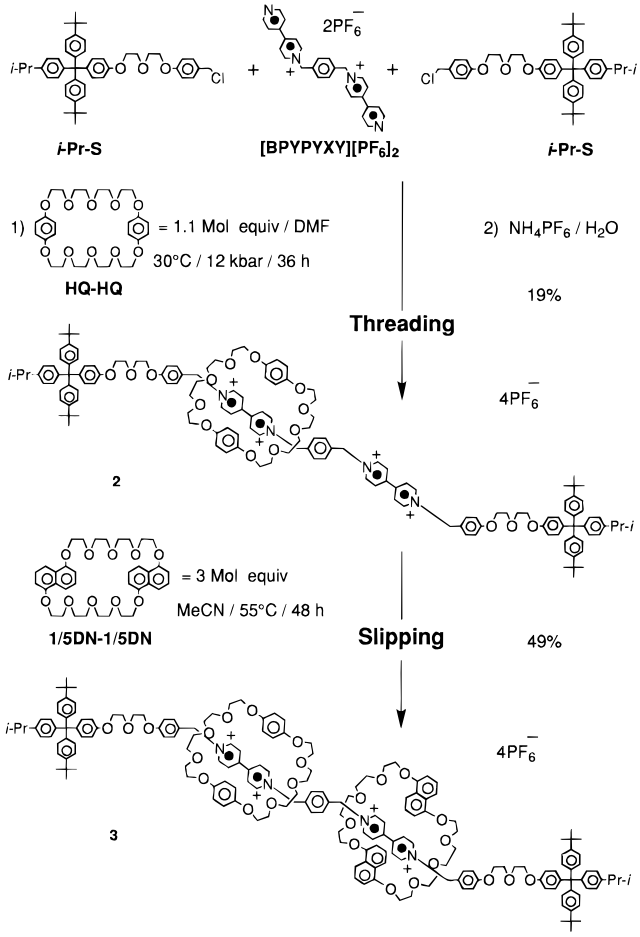

atoms on the bipyridinium units incorporated within the dumbbell-shaped compound ***i*-Pr-D** and the rotaxanes **1**, **2**, and **3** are listed in Table 1. The ^{1}H-NMR spectrum of a CD_3COCD_3 solution of the dumbbell-shaped compound ***i*-Pr-D**, recorded at room temperature, shows two doublets centered on δ 9.46 and 8.79 for the α- and β-protons, respectively. After the slipping-on of the 1,5-dioxynaphthalene **1/5DN-1/5DN** macrocycle over the stoppers of the dumbbell-shaped compound ***i*-Pr-D**, the ^{1}H-NMR spectrum of the resulting [2]rotaxane **1**, recorded in CD_3COCD_3 at room temperature, shows dramatic upfield shifts for both doublets. The resonance associated with the α-protons moves to δ 9.02, while the signal for the β-protons is shifted to δ 7.38. The expected upfield shift is a result of the shielding effect exerted by the two naphthalene rings *sandwiching* the bipyridinium unit within the [2]rotaxane structure. The ^{1}H-NMR spectrum of a CD_3COCD_3 solution of the [2]rotaxane **2** incorporating one **HQ-HQ** macrocycle, but having two bipyridinium units within the dumbbell-shaped component, shows only two doublets centered on δ 9.32 and 9.27 for the α-protons and two doublets centered on δ 8.47 and 8.44 for the β-protons when recorded at room temperature. The simplicity of the spectrum is a result of the *shuttling*[6] of the macrocyclic component back and forth from one bipyridinium recognition site to the other. This process is fast on the ^{1}H-NMR time scale at room temperature. Thus, the signals of the two bipyridinium *stations* are averaged and distinction between *occupied* and *unoccupied stations* is not possible at this temperature. Slipping-on of the **1/5DN-1/5DN** macrocycle over the stoppers of the [2]rotaxane **2** affords the [3]rotaxane **3** in which each bipyridinium unit is encircled by two constitutionally different macrocyclic components. As a result, the ^{1}H-NMR spectrum of the [3]rotaxane **3** shows four doublets centered on δ 9.16, 9.09, 9.05, and 9.00 for the α-protons, and one multiplet at δ 8.14-8.07 and two doublets centered on δ 7.39 and 7.33 for the β-protons, of the bipyridinium units.

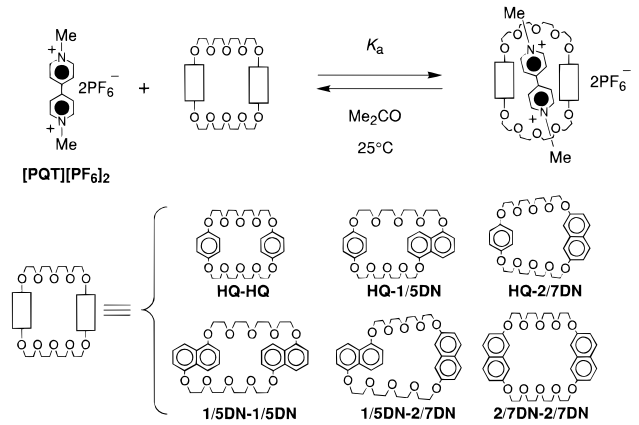

Figure 2. Complexation of **[PQT][PF$_6$]$_2$** by the π-electron-rich macrocyclic polyethers **HQ-HQ**, **HQ-1/5DN**, **HQ-2/7DN**, **1/5DN-1/5DN**, **1/5DN-2/7DN**, and **2/7DN-2/7DN**.

Table 1. Chemical Shifts[a] for the Protons in the α- and β-Positions with respect to the Nitrogen Atoms on the Bipyridinium Units Incorporated within the Dumbbell-Shaped Compound ***i*-Pr-D** and the Rotaxanes **1**, **2**, and **3**

compd	α-CH (δ)	β-CH (δ)
***i*-Pr-D**	9.46	8.79
1	9.02	7.38
2[b]	9.32, 9.27	8.47, 8.44
3[c]	9.16, 9.09, 9.05, 9.00	8.14−8.07, 7.39, 7.33

[a] The ^{1}H-NMR spectra were recorded at room temperature in CD_3COCD_3 on a Bruker AC300 (300 MHz) spectrometer. [b] The ^{1}H-NMR spectrum of **2** shows two pairs of doublets for the α-CH and β-CH protons. [c] The ^{1}H-NMR spectrum of **3** shows four doublets for the α-CH protons and one multiplet and two doublets for the β-CH protons.

Kinetic Studies. In order to gain further insight into the slipping approach to rotaxanes, it was decided to investigate the kinetics of these processes, changing systematically not only the size of the stoppers but also the size of the cavity of the macrocyclic components. The macrocyclic polyethers, depicted in Figure 2, incorporate π-electron-rich aromatic rings such as hydroquinone, 1,5-dioxynaphthalene, and/or 2,7-dioxynaphthalene and are able to bind[7] in solution the bipyridinium-based bis(hexafluorophosphate) salt **[PQT][PF$_6$]$_2$** with pseudorotaxane-like geometries. The association constants (Table 2) in Me_2CO at 25 °C range from 414 up to 1190 M^{-1} and were evaluated[7] by absorption UV−visible spectroscopy, employing

(6) In previous investigations, a free energy of activation ($\Delta G^{\ddagger}$) of *ca.* 10 kcal mol^{-1} at 215 K for the degenerate site-exchange process—namely, the *shuttling* of the macrocyclic component from one bipyridinium recognition site to the other—occurring within [2]rotaxanes incorporating either tris(4-*tert*-butylphenylmethyl groups (R = *t*-Bu) or phenylbis(4-*tert*-butylphenyl)methyl groups (R = H) as the stoppers was derived by the coalescence method. See refs 3b,e and: Ashton, P. R.; Philp, D.; Spencer, N.; Stoddart, J.F. *J. Chem. Soc., Chem. Commun.* **1992**, 1124−1128.

(7) (a) Allwood, B. L.; Spencer, N.; Shahriari-Zavareh, H.; Stoddart, J. F.; Williams, D. J. *J. Chem. Soc., Chem. Commun.* **1987**, 1064−1066. (b) Ashton, P. R.; Chrystal, E. J. T.; Mathias, J. P.; Parry, K. P.; Slawin, A. M. Z.; Spencer, N.; Stoddart, J. F.; Williams, D. J. *Tetrahedron Lett.* **1987**, *28*, 6367−6370. (c) Ortholand, J. Y.; Slawin, A. M. Z.; Spencer, N.; Stoddart, J. F.; Williams, D. J. *Angew. Chem., Int. Ed. Engl.* **1989**, *28*, 1394−1397. (d) Anelli, P. L.; Ashton, P. R.; Ballardini, R.; Balzani, V.; Delgado, M.; Gandolfi, M. T.; Goodnow, T. T.; Kaifer, A. E.; Philp, D.; Pietraszkiewicz, M.; Prodi, L.; Reddington, M. V.; Slawin, A. M. Z.; Spencer, N.; Stoddart, J. F.; Vicent, C.; Williams, D. J. *J. Am. Chem. Soc.* **1992**, *114*, 193−218. (e) Asakawa, M.; Ashton, P. R.; Boyd, S. E.; Brown, C. L.; Gillard, R. E.; Kocian, O.; Raymo, F. M; Stoddart, J. F.; Tolley, M. S.; Williams, D. J. *J. Org. Chem.* In press.

Table 2. Association Constants (K_a) and Free Energies of Complexation ($-\Delta G°$) for the Binding of **[PQT]PF$_6$]$_2$** by Macrocyclic Polyethers Incorporating π-Electron Rich Aromatic Units such as Hydroquinone, 1,5-Dioxynaphthalene, and/or 2,7-Dioxynaphthalene

compd	K_a (M^{-1})	$-\Delta G°$ (kcal mol^{-1})	λ_{max}[a] (nm)
HQ-HQ	730	3.90	435
HQ-1/5DN	919	4.04	456
HQ-2/7DN	414	3.57	416
1/5DN-1/5DN	1190	4.19	480
1/5DN-2/7DN	852	4.00	436
2/7DN-2/7DN	970	4.07	418

[a] Wavelength of the maximum of the charge-transfer band associated with the interaction between the π-electron-deficient bipyridinium unit and the π-electron-rich aromatic rings incorporated within the macrocyclic polyethers.

the charge-transfer band arising from the interaction between the π-electron-deficient bipyridinium unit and the π-electron-rich aromatic rings incorporated within the macrocycles.

In order to test the ability of these macrocyclic polyethers to slip-on over bis(4-*tert*-butylphenyl)-4-R-phenylmethane-based stoppers, each of the dumbbell-shaped compounds (Figure 3) **Et-D**, ***i*-Pr-D**, **cyclohexyl-D**, and ***t*-Bu-D** was mixed in CD_3CN solution with equimolar amounts of each macrocycle. The resulting solutions were heated at 50 °C and the self-assembly of the corresponding [2]rotaxanes was followed by monitoring the increasing absorbance A of the charge-transfer band associated with the newly formed [2]rotaxanes in the visible spectra. However, a constant value of A is achieved after a period of time, *i.e.* equilibrium between the [2]rotaxane and the *free* macrocyclic and dumbbell-shaped components is reached. Nonlinear curve fitting of the plot of A against time t can be achieved by employing eq 1:[8]

$$A = \frac{\epsilon\left[C_0^{\,2}C_e\left(1 - e^{k_{on}t\frac{(C_0^{\,2} - C_e^{\,2})}{C_e}}\right)\right]}{C_e^{\,2} - C_0^{\,2}e^{k_{on}t\frac{(C_0^{\,2} - C_e^{\,2})}{C_e}}} \qquad (1)$$

where A, ϵ, and t are absorbance, molar extinction coefficient, and time, respectively, C_0 is the initial concentration of the species, while C_e is the concentration of the [2]rotaxane at equilibrium, and k_{on} (Figure 1) is the rate constant of the slipping-on process. A and t are experimentally measurable, while C_0 is known. C_e can be determined[9] by recording the ^{1}H-NMR spectra of the solutions at the same temperature. The exchange between the *free* species and the [2]rotaxane is slow on the ^{1}H-NMR time scale. Thus, distinct resonances for the *free* species and the [2]rotaxane are observed in the spectra. Integration of these signals affords the C_e value and, as a result, ϵ can be determined ($A_e = \epsilon l C_e$, A_e is the absorbance at equilibrium and l is the optical path) by measuring the absorbance of the charge-transfer bands at saturation—*i.e.* at equilibrium. Hence, the only unknown is the rate constant k_{on} which can be calculated by using a nonlinear curve fitting program. By employing this methodology, the free energies of activation ($\Delta G^{‡}_{on}$ and $\Delta G^{‡}_{off}$) and of association ($\Delta G°$) listed in Table 3 for the slipping processes in CD_3CN at 50 °C, involving the dumbbell-shaped compounds **Et-D**, ***i*-Pr-D**, **cyclohexyl-D**, and ***t*-Bu-D**, were determined. As expected, in the case of **Et-D**, the free energies of activation $\Delta G^{‡}_{on}$ for the slipping-on process decrease by *ca.* 3.8 kcal mol^{-1} on going from the *small* **HQ-HQ** to the *large* **1/5DN-1/5DN** macrocycle (from left to right in Table 3). However, when the even *larger* macrocyclic polyether **1/5DN-2/7DN** is employed the equilibrium is reached immediately. In the case of ***i*-Pr-D**, no slipping-on occurs—*i.e.* no charge-transfer band is detected—when the **HQ-HQ** and **HQ-1/5DN** macrocycles are employed, suggesting that the size of the cavities of these two macrocycles is too

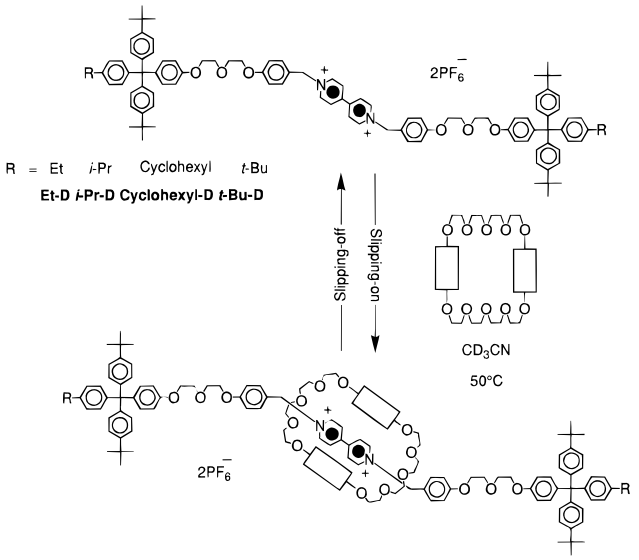

Figure 3. Slipping processes involving the π-electron rich macrocyclic polyethers **HQ-HQ**, **HQ-1/5DN**, **HQ-2/7DN**, **1/5DN-1/5DN**, **1/5DN-2/7DN**, and **2/7DN-2/7DN** and the π-electron-deficient dumbbell-shaped compounds **Et-D**, ***i*-Pr-D**, **cyclohexyl-D**, and ***t*-Bu-D**.

Table 3. Free Energies (kcal mol^{-1}) of Activation ($\Delta G^{‡}_{on}$ and $\Delta G^{‡}_{off}$) and of Association ($\Delta G°$) for the Slipping of the π-Electron Rich Macrocyclic Polyethers over the Stoppers of the π-Electron-Deficient Dumbbell-Shaped Compounds in CD_3CN at 50 °C

		macrocycles				
dumbbells	parameters	**HQ-HQ**[a]	**HQ-1/5DN**	**1/5DN-1/5DN**[a]	**HQ-2/7DN**	**1/5DN-2/7DN**
Et-D	$\Delta G^{‡}_{on}$[b]	24.5	22.4	21.3	20.7	*f*
	$\Delta G^{‡}_{off}$[c]	26.1	25.5	24.9	22.9	*f*
	$-\Delta G°$[d]	1.6	3.1	3.6	2.2	*f*
i-Pr-D	$\Delta G^{‡}_{on}$[b]	*e*	*e*	23.9	24.5	21.8
	$\Delta G^{‡}_{off}$[c]	*e*	*e*	28.6	26.6	24.4
	$-\Delta G°$[d]	*e*	*e*	4.7	2.1	2.6
cyclohexyl-D	$\Delta G^{‡}_{on}$[b]	*e*	*e*	*e*	*e*	24.2
	$\Delta G^{‡}_{off}$[c]	*e*	*e*	*e*	*e*	26.3
	$-\Delta G°$[d]	*e*	*e*	*e*	*e*	2.1

[a] The molar extinction coefficient (ϵ) values measured for one of the [2]rotaxanes depicted in Scheme 1 and the [2]rotaxane **1** in CD_3CN at 50 °C were employed to calculate the kinetic and thermodynamic parameters for the slipping of **HQ-HQ** and **1/5DN-1/5DN**, respectively, over the stoppers of the dumbbell-shaped compounds under these conditions. [b] Free energy of activation for the slipping-on process (percentage error ≤ 0.4%). [c] Free energy of activation for the slipping-off process (percentage error ≤ 1%). [d] Free energy of association (percentage error ≤ 5%). [e] No rotaxane formation occurs—*i.e.*, no charge-transfer band is detected. When the dumbbell-shaped compound ***t*-Bu-D** is employed in combination with the dumbbell-shaped compounds **Et-D**, ***i*-Pr-D**, and **cyclohexyl-D**, no rotaxane formation occurs. [f] The equilibrium was reached immediately. When the macrocyclic polyether **2/7DN-2/7DN** is employed in combination with any of the dumbbell-shaped components, the equilibrium is reached immediately.

(8) Equation 1 was determined as reported in the Supporting Information. For further information, see: Laidler, K. J. *Chemical Kinetics*; Harper Collins Publisher: New York, 1987.

(9) When the macrocyclic polyether **HQ-HQ** or **1/5DN-1/5DN** is employed, C_e can be calculated from the equation $A_e = \epsilon l C_e$, where l is the optical path and is equal to 1 cm, by measuring the absorbance at the equilibrium A_e and the molar extinction coefficient ϵ of one of the [2]rotaxanes shown in Scheme 1 or the [2]rotaxane **1**, respectively, under the same conditions of the experiment. The value of ϵ is not affected by the nature of the R groups linked to the tetraarylmethane-based stoppers. See ref 3e.

small for their passage over the "*i*-Pr-substituted" stoppers. However, when the *larger* macrocycles **HQ-2/7DN**, **1/5DN-1/5DN**, and **1/5DN-2/7DN** are employed, $\Delta G^{\ddagger}_{on}$ values of 23.9, 24.5, and 21.8 kcal mol^{-1}, respectively, are calculated. In the case of **cyclohexyl-D**, only the macrocycle **1/5DN-2/7DN** is able to slip-on over the "cyclohexyl-substituted" stoppers. No charge-transfer band was detected in the case of the smaller macrocycles. When the dumbbell-shaped compound ***t*-Bu-D** is employed, no charge-transfer band is detected for any of the macrocycles **HQ-HQ**, **HQ-1/5DN**, **1/5DN-1/5DN**, and **1/5DN-2/7DN**, suggesting that the "*t*-Bu-substituted" stoppers are too bulky to permit the passage of these macrocycles over them at 50 °C in CD_3CN. However, the macrocyclic polyether **2/7DN-2/7DN** possesses a cavity larger than that of any of the other macrocycles. Thus, when **2/7DN-2/7DN** is heated at 50 °C with any of the dumbbell-shaped compounds **Et-D**, ***i*-Pr-D**, **cyclohexyl-D**, and ***t*-Bu-D**, a charge-transfer band is detected and no change of its absorbance is observed with time, suggesting that the equilibrium is reached immediately in all cases. These results suggest that the energy barrier $\Delta G^{\ddagger}_{on}$ (Figure 1) for the slipping-on process is related to the size of the cavity of the macrocyclic polyether. Thus, the size and the substitution pattern of the two aromatic rings incorporated in each macrocycle should be capable of correlation to $\Delta G^{\ddagger}_{on}$. The C−C distances between the carbon atoms bearing the methoxy substituents and the O−O distances for the model compounds 1,4-dimethoxybenzene (**1/4DMB**), 1,5-dimethoxynaphthalene (**1/5DMN**), and 2,7-dimethoxynaphthalene (**2/7DMN**) are listed in Figure 4 and were determined by computer molecular modeling studies. Assuming that these values do not differ significantly for the dioxy-substituted aromatic rings incorporated in the macrocyclic polyethers, a parameter X_{C-C} can be defined for each macrocycle as the sum of the two C−C distance values for its two aromatic rings. Similarly, X_{O-O} can be defined as the sum of the two O−O distance values for the two dioxy-substituted aromatic rings of each macrocycle. A plot of the $\Delta G^{\ddagger}_{on}$ values listed in Table 3 for the slipping-on over the stoppers of the dumbbell-shaped compound **Et-D** against X_{C-C} is illustrated in Figure 4a, while Figure 4b shows a plot of the same $\Delta G^{\ddagger}_{on}$ values against X_{O-O}. In both cases, monotonic correlations between the energy barrier $\Delta G^{\ddagger}_{on}$ and the distance parameters X_{C-C} and X_{O-O} are observed.

In order to investigate the effect of temperature T upon these processes, the slipping of the macrocycle **1/5DN-1/5DN** over the stoppers of the dumbbell-shaped compound **Et-D** in CD_3CN was followed (Table 4) at four different temperatures—namely, 30, 40, 50, and 60 °C. The enthalpic (ΔH) and entropic ($-T\Delta S$) contributions (Table 4) to the free energy values were determined from the straight line plots of the free energies against T. In the case of the free energy of activation ($\Delta G^{\ddagger}_{on}$) for the slipping-on process, a small difference between enthalpic and entropic contributions is observed. On the contrary, in the case of the free energy of activation ($\Delta G^{\ddagger}_{off}$) for the slipping-off process, the enthalpic contribution is predominant ($\Delta H^{\ddagger}_{off} > -T\Delta S^{\ddagger}_{off}$). The strong noncovalent bonding interactions between the π-electron-rich macrocycle and the π-electron-deficient bipydinium recognition site have to be destroyed in order to dismember the [2]rotaxane. Thus, the slipping-off process is enthalpically demanding.

The slippage of the macrocycle **1/5DN-1/5DN** over the stoppers of the dumbbell-shaped compound **Et-D** was followed in a range of solvents at 30 °C. The resulting free energies of activation ($\Delta G^{\ddagger}_{on}$ and $\Delta G^{\ddagger}_{off}$) and of asscociation ($\Delta G°$) are listed in Table 5. The free energy of activation ($\Delta G^{\ddagger}_{on}$) for the slipping-on processes range over about 1 kcal mol^{-1}, increasing on going from $(CD_3)_2CO$ to DMF-d_7 (from left to right in Table 5). Interestingly, when the low polar solvents $CDCl_3$ and CD_2Cl_2 are employed, the equilibrium is reached immediately—*i.e.* a charge-transfer band of constant intensity with time is detected.

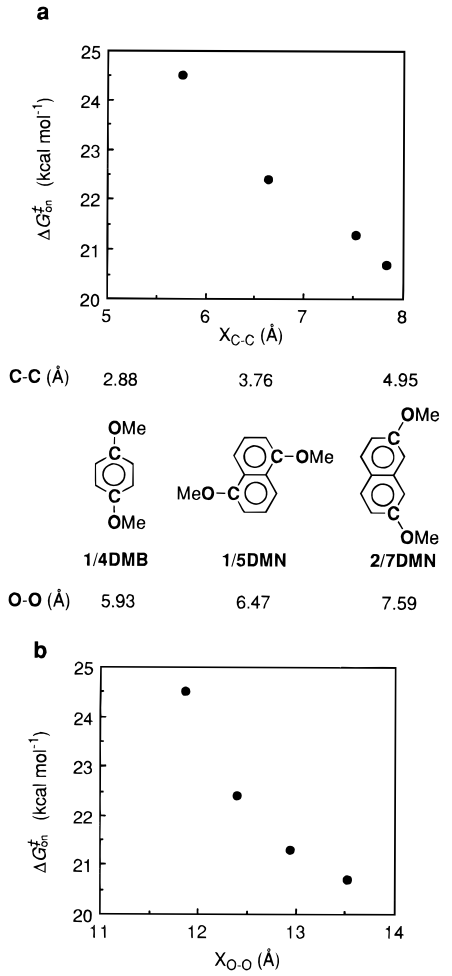

Figure 4. Correlation between the free energy of activation ($\Delta G^{\ddagger}_{on}$) associated with the slipping-on processes and the distance parameters (a) X_{C-C} and (b) X_{O-O}.

Table 4. Enthalpic and Entropic Contributions to the Free Energies (kcal mol^{-1}) of Activation ($\Delta G^{\ddagger}_{on}$ and $\Delta G^{\ddagger}_{off}$) and of Association ($\Delta G°$) for the Slipping of the Macrocyclic Polyether **1/5DN-1/5DN**[a] over the Stoppers of the Dumbbell-Shaped Compound **Et-D** in CD_3CN at Various Temperatures

parameters	30 °C	40 °C	50 °C	60 °C
$\Delta G^{\ddagger}_{on}$[b]	20.7	21.1	21.3	21.8
$-\Delta H^{\ddagger}_{on}$[c]	10.1	10.1	10.1	10.1
$-T\Delta S^{\ddagger}_{on}$[d]	10.6	11.0	11.2	11.7
$\Delta G^{\ddagger}_{off}$[e]	24.6	24.8	24.9	25.0
$\Delta H^{\ddagger}_{off}$[f]	20.7	20.7	20.7	20.7
$-T\Delta S^{\ddagger}_{off}$[g]	3.9	4.1	4.2	4.3
$-\Delta G°$[h]	3.9	3.7	3.6	3.2
$-\Delta H°$[i]	10.0	10.0	10.0	10.0
$T\Delta S°$[j]	6.1	6.3	6.4	6.6

[a] The molar extinction coefficient (ϵ) values measured for the [2]rotaxane **1** in CD_3CN at 50 °C were employed to calculate the kinetic and thermodynamic parameters for the slipping of **1/5DN-1/5DN** over the stoppers of **Et-D**. [b] Free energy of activation for the slipping-on process (percentage error ≤ 0.03%). [c] Enthalpic contribution to $\Delta G^{\ddagger}_{on}$ (percentage error ≤ 50%). [d] Entropic contribution to $\Delta G^{\ddagger}_{on}$ (percentage error ≤ 49%). [e] Free energy of activation for the slipping-off process (percentage error ≤ 0.07%). [f] Enthalpic contribution to $\Delta G^{\ddagger}_{off}$ (percentage error ≤ 12%). [g] Entropic contribution to $\Delta G^{\ddagger}_{off}$ (percentage error ≤ 62%). [h] Free energy of association (percentage error ≤ 0.3%). [i] Enthalpic contribution to $\Delta G°$ (percentage error ≤ 45%). [j] Entropic contribution to $\Delta G°$ (percentage error ≤ 50%).

Table 5. Free Energies (kcal mol^{-1}) of Activation ($\Delta G^{\ddagger}_{on}$ and $\Delta G^{\ddagger}_{off}$) and of Association ($\Delta G°$) for the Slipping of the Macrocyclic Polyether **1/5DN-1/5DN** over the Stoppers of the Dumbbell-Shaped Compound **Et-D** in Various Solvents at 30 °C

parameters	$CDCl_3$[a,b]	CD_2Cl_2[a,b]	$(CD_3)_2CO$	CD_3CN	CD_3NO_2	$(CD_3)_2SO$[a]	THF-d_8	DMF-d_7[a]
$\Delta G^{\ddagger}_{on}$[c]	<20	<20	20.4	20.7	21.0	21.1	21.3	21.4
$\Delta G^{\ddagger}_{off}$[d]	<23	<23	25.2	24.6	24.4	22.6	26.1	23.6
$-\Delta G°$ [e]	2.9	3.6	4.8	3.9	3.4	1.5	4.8	2.2

[a] The molar extinction coefficient (ϵ) values measured for the [2]rotaxane **1** in each of the solvents listed were employed to calculate the kinetic and thermodynamic parameters for the slipping of **1/5DN-1/5DN** over the stoppers of **Et-D** in these solvents. [b] In $CDCl_3$ and CD_2Cl_2, the equilibrium is reached immediately, *i.e.*, a value constant in time for the absorbance of the charge transfer band associated with the resulting [2]rotaxane **1** is measured. This result suggests that the values of $\Delta G^{\ddagger}_{on}$ in $CDCl_3$ and CD_2Cl_2 are lower than those measured in any other of the solvents listed in the table. [c] Free energy of activation for the slipping-on process (percentage error ≤ 0.06%). [d] Free energy of activation for the slipping-off process (percentage error ≤ 0.2%). [e] Free energy of association (percentage error ≤ 0.8%).

These results suggest that, presumably, the macrocyclic polyether and/or the dumbbell-shaped compound are highly solvated in a solvent such as DMF-d_7. Thus, desolvation is required in order to slip-on the macrocycle over the stoppers, resulting in a high energy of activation ($\Delta G^{\ddagger}_{on}$). On the contrary, presumably as a result of the low degree of solvation in nonpolar solvents, low values of the energies of activation ($\Delta G^{\ddagger}_{on}$ and $\Delta G^{\ddagger}_{off}$) are achieved in $CDCl_3$ and CD_2Cl_2. An approximately opposite behavior is observed for the free energy of activation ($\Delta G^{\ddagger}_{off}$) for the slipping-off processes. The lowest value (22.6 kcal mol^{-1}) for $\Delta G^{\ddagger}_{off}$ is measured in the highly polar solvent $(CD_3)_2SO$, while the highest value (26.1 kcal mol^{-1}) for $\Delta G^{\ddagger}_{off}$ is observed in THF-d_8. These results are directly reflected in the values of the free energy of association ($\Delta G°$), which reach a maximum when either THF-d_8 or $(CD_3)_2CO$ is employed. In other words, THF-d_8 and $(CD_3)_2CO$ seem to be the *best* solvents for the self-assembly of these [2]rotaxanes: a relatively fast slipping-on process is observed in addition to a high free energy of association—thus, leading to a high yield of the [2]rotaxane. The free energy of association ($\Delta G°$) and the free energies of activation ($\Delta G^{\ddagger}_{on}$ and $\Delta G^{\ddagger}_{off}$) were plotted against the dipole moments,[10] the dielectric constants,[10] donor numbers,[11] and *Z*-values[12] of the solvents. However, no significant correlations between these values were observed.

Spectroscopic and Electrochemical Properties. The rotaxanes incorporate a number of chromophoric and electroactive units, and as a result, they exhibit very interesting spectroscopic and electrochemical properties. In particular, the [3]rotaxane **3** (Figure 5), which is made of the dumbbell-shaped component **5** and the two macrocycles **HQ-HQ** and **1/5DN-1/5DN**, incorporates altogether as many as ten chromophoric and electroactive units—namely, two 1,4-dimethoxybenzene-like units (**1/4DMB**) and two 1,5-dimethoxynaphthalene-like units (**1/5DMN**) in the two macrocyclic components, and two tetraarylmethane-like stoppers (**R-S**), two methoxybenzene-like units (**MB**), and two paraquat-like units (**PQT**) in the dumbbell-shaped component **5**. It is important to notice that, whereas the R groups attached to the stoppers play a most important role in the kinetics of the slippage processes, they do not have any effect on the absorption spectra, luminescence properties, and electrochemical behavior.[3e] This is the reason why the R groups attached to the stoppers are not indicated in Figure 5 and are not mentioned in the following discussion. The spectroscopic and electrochemical data of the **1/5DN-1/5DN** macrocycle, [2]rotaxane **1,** and [3]rotaxane **3** are listed in Table 6, together with the previously obtained results for the **HQ-HQ** macrocycle.[3e,7d]

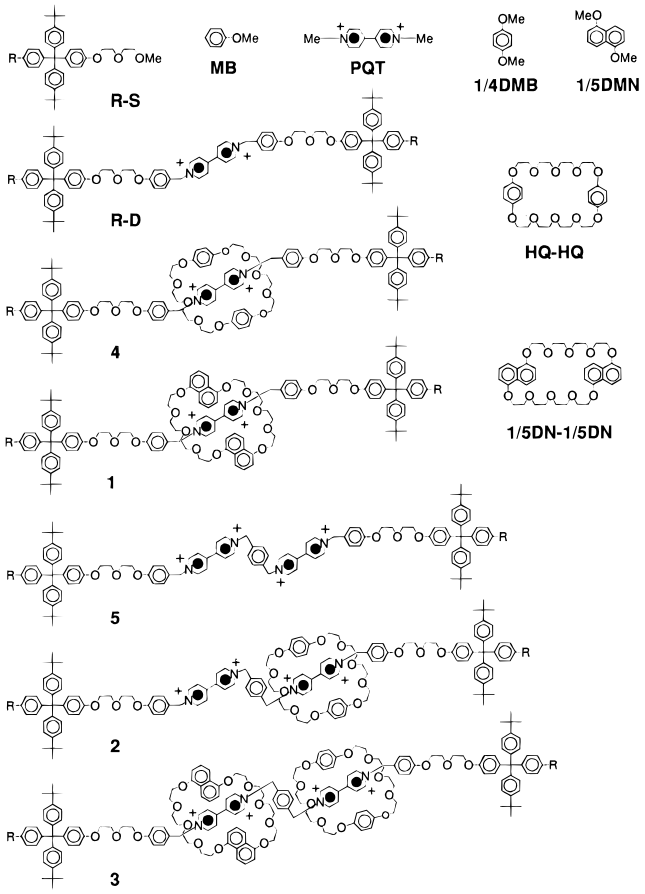

Figure 5. Macrocycles, dumbbell-shaped compounds, rotaxanes, and model compounds employed in the photochemical and electrochemical investigations.

(a) Spectroscopic Properties. In agreement with the behavior exhibited by analogous rotaxanes,[3e] the [2]rotaxane **1** and the [3]rotaxane **3** show in the visible region a weak (and broad in the case of **3**) absorption band (Table 6) due to the charge-transfer (CT) interaction between the electron-donor units (**1/4DMB** and/or **1/5DMN**) of the macrocycles and the electron-acceptor units (**PQT**) present in their dumbbell-shaped components. With respect to the [2]rotaxane **4**,[3e] the CT absorption band of **1** lies at lower energy, since **1/5DN-1/5DN** is a better electron donor than **HQ-HQ**. In the [3]rotaxane **3** two different macrocycles are present and therefore two CT bands are expected. A closer analysis of the broad absorption band of **3** shows, indeed, that there are two components. Subtraction of the spectrum of previously studied the [2]rotaxane **2**[3e] (which contains two **PQT** stations and only **HQ-HQ** macrocycle) from the spectrum of **3** gives an absorption band almost identical to that exhibited by the [2]rotaxane **1**, where a **PQT** unit is engaged with a **1/5DN-1/5DN** macrocycle.

(10) Riddick, J. A.; Bunger, W. B. *Organic Solvents, Techniques of Chemistry;* Wiley: New York, 1970; Vol. 2.

(11) Reichardt, C. *Solvents and Solvent Effects in Organic Chemistry*; VCH: Weinheim, 1988.

(12) (a) Kosower, E. M. *J. Am. Chem. Soc.* **1958**, *80*, 3253−3260. (b) Kosower, E. M. *J. Am. Chem. Soc.* **1958**, *80*, 3261−3267. (c) Kosower, E. M. *J. Am. Chem. Soc.* **1958**, *80*, 3267−3270.

Table 6. Spectroscopic and Electrochemical Data for the Macrocycles **HQ-HQ** and **1/5DN-1/5DN**, the [2]Rotaxane **1**, and the [3]Rotaxane **3** in MeCN at Room Temperature

	absorption		fluorescence			reduction[a] V *vs* SCE		oxidation[b] V *vs* SCE
compd	λ (nm)	ϵ ($M^{-1}cm^{-1}$)	λ (nm)	τ (ns)	ϕ			
HQ-HQ[c]	290	5200	320	2.5	0.08			+1.28 (**1/4DMB**)
1/5DN-1/5DN	295	17600	330	8.5	0.27			+1.01 (**1/5DMN**)
1	270	33500	*d*		*d*	−0.52	−0.89	+1.29 (**1/5DMN**)
	313	11000						
	326	9400						
	507	700						
3	269	59000	*d*		*d*	−0.46[e,f]	−0.87[e,g]	+1.32 (**1/5DMN**)
	325	11500						+1.41 (**1/4DMB**)
	479	1100						

[a] Halfwave potential values; unless otherwise noted, the reduction processes are reversible and monoelectronic. [b] Potential values evaluated from the DPV peaks; the unit involved in the oxidation process is reported in parentheses. [c] Literature values (Anelli, P. L.; Ashton, P. R.; Ballardini, R.; Balzani, V.; Delgado, M.; Gandolfi, M. T.; Goodnow, T. T.; Kaifer, A. E.; Philp, D.; Pietraszkiewicz, M.; Prodi, L.; Reddington, M. V.; Slawin, A. M. Z.; Spencer, N.; Stoddart, J. F.; Vicent, C.; Williams, D. J. *J. Am. Chem. Soc.* **1992**, *114*, 193−218. Ashton, P. R.; Ballardini, R.; Balzani, V.; Belohradsky, M.; Gandolfi, M. T.; Philp, D.; Prodi, L.; Raymo, F. M.; Reddington, M. V.; Spencer, N.; Stoddart, J. F.; Venturi, M.; Williams, D. J. *J. Am. Chem. Soc.* **1996**, *118*, 4931−4951). [d] Fluorescence from a very small amount of free **1/5DN-1/5DN** precludes the observation of the very weak stopper fluorescence (see text). [e] Bielectronic process. [f] The potential values of the two monoelectronic processes are −0.44 and −0.49 V (see text). [g] The potential values of the two monoelectronic processes are −0.85 and −0.90 V.

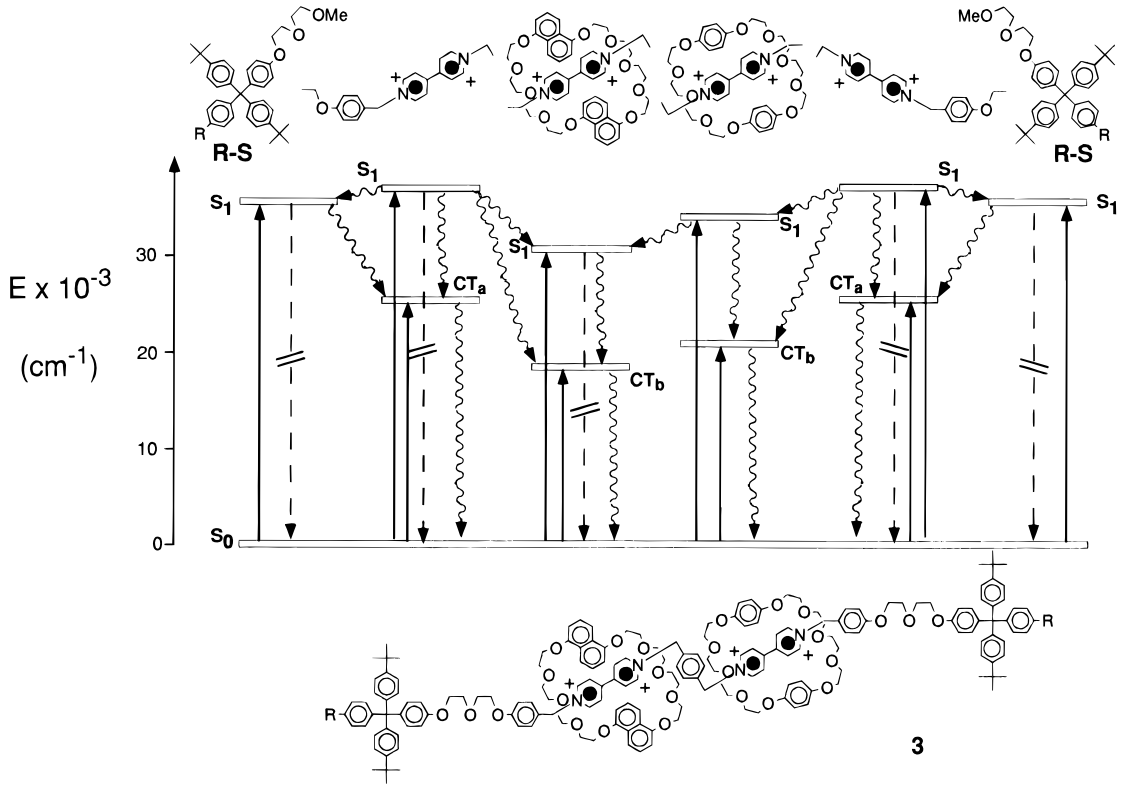

Figure 6. Simplified energy-level diagram of the [3]rotaxane **3**. The energies of the CT levels have been estimated from the maxima of the absorption bands and the energies of the S_1 levels have been estimated from the onset of the emission spectra.

The CT interaction between the macrocycles and the **PQT** units of the dumbbell-shaped components is also responsible for the fact that the luminescence properties of **1** and **3** (Table 6) are completely different from those of their separated components. The CT excited states, in fact, lying below the fluorescent levels of the **HQ-HQ** and **1/5DN-1/5DN**, introduce fast radiationless deactivation routes which lead to a complete quenching of the strong emission of the macrocycles. Whether or not the very weak fluorescence of the **R-S** units observed for the dumbbell-shaped components[3e] is still present in **1** and **3** cannot be said because of the presence of an interfering impurity emission. A simplified energy-level diagram of the [3]rotaxane **3** is illustrated schematically in Figure 6.

(b) Electrochemical Properties. In Figure 7 the $E_{1/2}$ values concerning the reduction of the **PQT** units of the [2]rotaxane **1** and the [3]rotaxane **3** are correlated with those previously obtained[3e] for dumbbell-shaped components **R-D** and **5** and the [2]rotaxanes **2** and **4**. In the case of the [3]rotaxane **3**, because of the different electron-donor ability of the two macroclycles, four monoelectronic reduction processes are expected. It should also be noted, however, that the reduction of the **PQT** unit in **1** is only slightly shifted toward more negative potentials compared to **4** ($\Delta E_{1/2} = 50$ and 20 mV for the first and second reduction process, respectively; Figure 7). Therefore, in **3**, the first two and the second two reductions might be expected to appear as unresolved processes. This expectation is confirmed by the experimental results, particularly by the differential pulse voltammogram which exhibits two broad, bielectronic peaks. With the reasonable assumption that the reduction potentials of the **PQT** unit surrounded by **HQ-HQ** are identical in **2** and **3**, the treatment of the differential pulse voltammetric peaks given by Richardson and Taube[13] allows us to obtain $E_{1/2}$ values

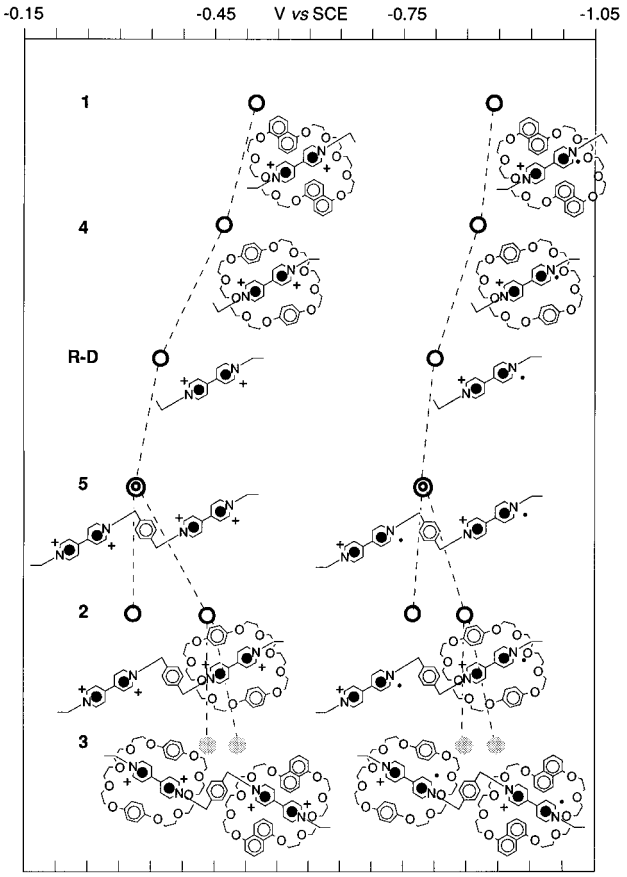

Figure 7. Correlations of the halfwave reduction potentials of the rotaxanes and their dumbbell-shaped components. Argon-purged MeCN solution. Bielectronic process (bold concentric circles); calculated values of the monoelectronic processes (shaded circle).

of −0.44, −0,49, −0,85, and −0,90 V *vs* SCE for the four one-electron processes of **3** (Table 6 and Figure 7). Looking at Figure 7, one can also note quantitative (considering the experimental error) correlations among all the reduction processes, particularly for the first reduction of each **PQT** unit. For example, **1/5DN-1/5DN** has the same effect on the first reduction of the **PQT** unit in **1** and **3**, *i.e.* shifts of 150 mV toward more negative potential in going from **R-D** to **1** and 160 mV in going from **5** to **3** are observed.

Although oxidations are not fully reversible, a correlation can be attempted, at least for the potentials of the first observed processes. On the basis of the results obtained for the [2]rotaxanes **2** and **4**,[3e] in **1** the first process, that occurs at less positive potential than in **2** and **4**, can be assigned to the oxidation of the **1/5DN-1/5DN** macrocycle, easier to oxidize than **HQ-HQ** (Table 6). In **3**, where both the **1/5DN-1/5DN** and **HQ-HQ** macrocycles are present, the first and second processes can be assigned to the oxidation of **1/5DN-1/5DN** and **HQ-HQ**, respectively, by comparison with the potential values of **1** and **4** (or **2**).

Conclusions

We have developed a synthetic approach—namely that of the slippage—to self-assembling [*n*]rotaxanes incorporating π-electron-deficient bipyridinium-based dumbbell-shaped components and π-electron-rich hydroquinone-, 1,5-dioxynaphthalene-, and/or 2,7-dioxynaphthalene-based macrocyclic polyether components. A systematic investigation of the kinetics of these self-assembly processes, performed while varying the size of both the macrocycle and the stoppers, has demonstrated that the size complementarity between the components is the major requirement for success in the slippage approach to rotaxanes. Indeed, only when the macrocyclic compound possesses a cavity large enough for it to slip over the bulky stoppers covalently attached at the ends of the dumbbell-shaped compound is rotaxane formation observed. Furthermore, the kinetic investigation of slippage, performed over a range of temperatures and in various solvents, has demonstrated that the enthalpic and entropic contributions to the free energy of activation associated with the second-order slipping-on process—namely the self-assembly of the rotaxane—are approximately the same, while the opposite slipping-off process—namely the dismembering of the rotaxane—is mainly enthalpically demanding. Also, the polarity of the solvent is reflected in the rates of both slipping-on and slipping-off processes suggesting that solvation of the components has a significant effect on the kinetics of these processes. These results suggest strongly the possibility of constructing complex molecular assemblies by carefully selecting appropriate building blocks and self-assembly approaches. Indeed, a [3]rotaxane, incorporating a π-electron deficient dumbbell-shaped component, comprised of two bipyridinium recognition sites, and encircled by two constitutionally different macrocyclic polyethers, was self-assembled in good yield. This [3]rotaxane incorporates altogether as many as ten chromophoric and electroactive sub-units and its spectroscopic and electrochemical properties and those of the related [2]rotaxane **1** and model compounds have been described and discussed. The two charge-transfer bands originating from the interaction between the electron-acceptor dumbbell-shaped component and the two different electron-donor macrocycles have been resolved. Correlations among the redox potentials of the various compounds have allowed the assignement of the reduction and oxidation processes to specific electroactive components.

Experimental Section

General Methods. Chemicals were purchased from Aldrich and used as received. Solvents were dried [MeCN (from P_2O_5), DMF (from CaH_2)] according to literature procedures.[14] The macrocyclic polyethers **HQ-HQ**,[7d] **HQ-1/5DN**,[7e] **HQ-2/7DN**,[7e] **1/5DN-1/5DN**,[7b] **1/5DN-2/7DN**,[7e] and **2/7DN-2/7DN**,[7e] the bis(hexafluorophosphate) salt **[BPYPYXY][PF$_6$]$_2$**,[7d] the tetrarylmethane-based stopper ***i*-Pr-S**, and the dumbbell-shaped compounds **Et-D**,[3e] ***i*-Pr-D**,[3e] **cyclohexyl-D**,[3e] and ***t*-Bu-D**[3e] were prepared according to published procedures. Reactions requiring ultrahigh pressures were carried out in Teflon vessels using a custom-built ultrahigh pressure reactor manufactured by PSIKA Pressure Systems Limited of Glossop, UK. Thin layer chromatography (TLC) was carried out on aluminium sheets coated with silica gel 60 (Merck 5554). Column chromatography was performed on silica gel 60 (Merck 9385, 230−400 mesh). Melting points were determined on an Electrothermal 9200 melting point apparatus and are uncorrected. Liquid secondary ion mass spectrometry (LSIMS) in conjunction with a 3-nitrobenzyl alcohol or 2-nitrophenyl octyl ether matrix was performed on a VG Prospec instrument. Electrospray positive-ion mass spectra (ESMS) were also measured on the VG Prospec mass spectrometer. UV−visible spectra were obtained and reaction kinetics followed by means of a computer-controlled Perkin-Elmer Lambda 2 spectrophotometer fitted with a thermostatic temperature controller (±0.2 °C). ^{1}H-NMR spectra were recorded on a Bruker AC300 (300 MHz) spectrometer. ^{13}C-NMR spectra were recorded on a Bruker AC300 (75 MHz) spectrometer.

[2]Rotaxane 1. A solution of ***i*-Pr-D** (108.0 mg, 0.06 mmol) and **1/5DN-1/5DN** (21.0 mg, 0.03 mmol) in dry MeCN (3 mL) was stirred at 50 °C for 24 h. The solvent was removed *in vacuo* and the residue was purified by column chromatography (SiO_2, MeOH/CH_2Cl_2/$MeNO_2$/2 M NH_4Cl, 6:2:1:0.2). The resulting purple solid was

(13) Richardson, D. E.; Taube, H. *Inorg. Chem.* **1981**, *20*, 1278−1285.

(14) Furniss, B. S.; Hannaford, A. J.; Smith, P. W. G. A.; Tatchell, R. *Practical Organic Chemistry*, Longman: New York, 1989.

dissolved in H_2O/$(Me)_2CO$ and a saturated aqueous solution of NH_4PF_6 was added. After the evaporation of the $(Me)_2CO$ under reduced pressure, a purple solid precipitated. The solid was filtered and washed with H_2O to give **2** (41.1 mg, 57%): mp 146 °C dec; LSIMS *m/z* 2272 $[M - PF_6]^+$, 2128 $[M - 2PF_6]^+$; ESMS: *m/z* 2272 $[M - PF_6]^+$; ^{1}H-NMR (CD_3COCD_3) δ 9.02 (4H, d, $J = 7$ Hz), 7.88 (4H, d, $J = 9$ Hz), 7.38 (4H, d, $J = 7$ Hz), 7.30−7.19 (12H, m), 7.14−7.04 (16H, m), 7.01 (4H, d, $J = 9$ Hz), 6.72 (4H, d, $J = 9$ Hz), 6.70−6.50 (8H, m), 6.45 (4H, d, $J = 7$ Hz), 6.02 (4H, s), 4.23−4.18 (4H, m), 4.04−3.91 (32H, m), 3.87−3.75 (12H, m), 2.90−2.81 (2H, m), 1.28 (36H, s), 1.20 (12H, d, $J = 7$ Hz); ^{13}C-NMR (CD_3CN) δ 161.3, 157.5, 154.0, 149.3, 147.1, 145.8, 145.4, 144.5, 140.5, 132.5, 132.2, 131.4, 131.1, 126.6, 126.4, 126.4, 126.0, 125.3, 124.9, 116.5, 114.1, 114.0, 106.6, 106.1, 71.9, 71.7, 71.4, 70.8, 70.3, 70.1, 68.9, 68.2, 65.3, 63.9, 34.8, 34.1, 31.5, 24.1. Anal. Calcd for $C_{140}H_{162}F_{12}N_2O_{16}P_2 \cdot H_2O$: C, 69.01; H, 6.78; N, 1.15. Found: C, 68.99; H, 7.09; N, 1.15.

[2]Rotaxane 2. A solution of ***i*-Pr-S** (300.0 mg, 0.43 mmol), **HQ-HQ** (124.0 mg, 0.23 mmol), and **[BPYPYXY][PF$_6$]$_2$** (150.0 mg, 0.20 mmol) in dry DMF (10 mL) was subjected to a pressure of 12 kbar at 30 °C for 36 h. The solvent was removed in vacuo and the resulting residue was washed with Et_2O (60 mL) and then dissolved in H_2O/$(Me)_2CO$ (200 mL). An aqueous solution of NH_4PF_6 was added and, after the evaporation of $(Me)_2CO$, a red solid precipitated. The solid was filtered off and purified by column chromatography (SiO_2, MeOH/CH_2Cl_2/$MeNO_2$/2 M NH_4Cl, 6:2:1:0.2) to give, after counterion exchange [H_2O/$(Me)_2CO$, saturated aqueous solution of NH_4PF_6] **2** as a red solid (111.2 mg, 19%): mp 220 °C dec; LSIMS *m/z* 2721 $[M - PF_6]^+$, 2576 $[M - 2PF_6]^+$; ESMS *m/z* 1290 $[M - 2PF_6]^{2+}$; ^{1}H-NMR (CD_3COCD_3) δ 9.32 (4H, d, $J = 7$ Hz), 9.24 (4H, d, $J = 7$ Hz), 8.47 (4H, d, $J = 7$ Hz), 8.44 (4H, d, $J = 7$ Hz), 7.91 (4H, s), 7.68 (4H, d, $J = 9$ Hz), 7.30 (8H, d, $J = 9$ Hz), 7.18−7.05 (24H, m), 6.82 (4H, d, $J = 9$ Hz), 6.19 (4H, s), 6.05 (12H, s), 4.21 (4H, t, $J = 5$ Hz), 4.12 (4H, t, $J = 5$ Hz), 3.92−3.85 (8H, m), 3.81−3.70 (24H, m), 3.64−3.61 (8H, m), 2.93−2.80 (2H, m), 1.29 (36 H, s), 1.22 (12 H, d, $J = 7$ Hz); ^{13}C-NMR (CD_3CN) δ 161.3, 157.8, 153.2, 149.6, 149.0, 147.4, 146.7, 146.4, 146.0, 145.6, 140.9, 135.8, 132.8, 132.6, 131.6, 131.4, 127.5, 127.3, 126.6, 125.7, 125.5, 116.6, 115.8, 114.45, 71.5, 71.3, 70.8, 70.6, 70.4, 68.9, 68.6, 68.5, 65.3, 65.0, 64.2, 35.1, 34.3, 31.7, 24.3. Anal. Calcd for $C_{150}H_{174}F_{24}N_4O_{16}P_4$: C, 62.80; H, 6.11; N, 1.95. Found: C, 62.95; H, 6.20; N, 1.95.

[3]Rotaxane 3. A solution of **2** (45.0 mg, 0.02 mmol) and **1/5DN-1/5DN** (40.0 mg, 0.06 mmol) in dry MeCN (3 mL) was stirred at 50 °C for 48 h. The solvent was removed in vacuo and the red residue was purified by column chromatography (SiO_2, MeOH/CH_2Cl_2/$MeNO_2$/2 M NH_4Cl, 6:2:1:0.2) to give, after counterion exchange [H_2O/$(Me)_2CO$, saturated aqueous solution of NH_4PF_6], **3** as a red solid (27.0 mg, 49%): mp 134 °C dec; LSIMS *m/z* 3360 $[M - PF_6]^+$, 3215 $[M - 2PF_6]^+$; ESMS *m/z* 1609 $[M - 2PF_6]^{2+}$, 1024 $[M - 3PF_6]^{3+}$; ^{1}H-NMR (CD_3COCD_3) δ 9.16 (2H, d, $J = 7$ Hz), 9.09 (2H, d, $J = 7$ Hz), 9.05 (2H, d, $J = 7$ Hz), 9.00 (2H, d, $J = 7$ Hz), 8.28−8.15 (4H, m), 8.14−8.07 (4H, m), 7.91 (2H, d, $J = 9$ Hz), 7.70 (2H, d, $J = 9$ Hz), 7.39 (2H, d, $J = 7$ Hz), 7.35−7.22 (12H, m), 7.19−7.03 (22H, m), 6.87−6.76 (4H, m), 6.72−6.63 (4H, m), 6.60−6.48 (8H, m), 6.22 (2H, s), 6.18 (2H, s), 6.09 (2H, s), 6.02−5.96 (10H, m), 4.24−4.17 (4H, m), 4.14−3.54 (76H, m), 2.93−2.79 (2H, m), 1.29 (18H, s), 1.28 (18H, s), 1.22 (6H, d, $J = 7$ Hz), 1.21 (6H, d, $J = 7$ Hz); ^{13}C-NMR (CD_3CN) δ 154.1, 152.9, 149.5, 147.3, 146.4, 145.5, 145.0, 140.8, 136.1, 132.8, 132.6, 132.5, 132.2, 132.0, 131.5, 131.3, 126.8, 126.5, 126.1, 125.4, 125.2, 125.0, 118.3, 116.6, 116.4, 115.6, 114.4, 114.0, 106.3, 72.0, 71.8, 71.3, 71.2, 70.9, 70.7, 70.5, 70.3, 69.0, 68.8, 68.5, 68.4, 64.1, 35.0, 34.2, 31.6, 24.3. Anal. Calcd for $C_{186}H_{218}F_{24}N_4O_{26}P_4$: C, 63.73; H, 6.27; N, 1.60. Found: C, 63.57; H, 6.40; N, 1.62.

General Method for the Determination of the Rate Constants. Equimolar amounts of a dumbbell-shaped compound and a macrocyclic polyether were dissolved in one of the deuterated solvents, preheated at temperature *T*, listed in Table 5 to afford a solution of known concentration C_0. The solution was mantained at temperature *T* by means of a thermostatic water bath over a period of time (*t*) and the absorbance (*A*) of the developing charge-transfer band associated with the resulting [2]rotaxane was monitored by absorption UV−visible spectroscopy. Heating was continued further until no change in the absorbance was detected—*i.e.* until the equilibrium was reached. At this juncture, an ^{1}H-NMR spectrum of the solution was recorded at the same temperature *T*. By integrating the resonances appearing in the ^{1}H-NMR spectrum associated with the [2]rotaxane and the *free* macrocyclic and dumbbell-shaped components, the concentration of the [2]rotaxane at equilibrium C_e was evaluated.[9] As a result, the molar extinction coefficient ϵ of the [2]rotaxane was calculated from the expression $A_e = \epsilon l C_e$, where A_e is the absorbance measured at equilibrium and *l* the optical path. By employing a nonlinear curve-fitting program, the plot of *A* against time (*t*) was fitted by eq 1[8] thus, affording the value of the rate constant k_{on} for the slipping-on process.

$$A = \frac{\epsilon\left[C_0^{\,2}C_e\left(1 - e^{k_{on}t\frac{(C_0^{\,2} - C_e^{\,2})}{C_e}}\right)\right]}{C_e^{\,2} - C_0^{\,2}e^{k_{on}t\frac{(C_0^{\,2} - C_e^{\,2})}{C_e}}} \qquad (1)$$

Absorption and Luminescence Measurements. Room temperature experiments were carried out in MeCN solutions. Electronic absorption spectra were recorded with a Perkin-Elmer λ6 spectrophotometer. Emission spectra were obtained with a Perkin-Elmer LS50 spectrofluorimeter. Emission spectra in butyronitrile rigid matrix at 77 K were recorded using quartz tubes immersed in a quartz Dewar filled with liquid nitrogen. Fluorescence quantum yields were determined using naphthalene in degassed cyclohexane as a standard ($\Phi = 0.23$).[15] Nanosecond lifetime measurements were performed with a previously described Edinburgh single-photon counting equipment.[16] Experimental errors: absorption maxima, ±2 nm; emission maxima, ±2 nm; excited state lifetimes, ±10%; fluorescence quantum yields, ±20%.

Electrochemical Measurements. Electrochemical experiments were carried out in argon-purged MeCN solution with a Princeton Applied Research 273 multipurpose instrument interfaced to a personal computer, using cyclic voltammetry (CV) and differential pulse voltammetry (DPV) techniques. The exact configuration and procedures for these measurements have been previously reported.[3e]

Acknowledgment. This research was supported by the Engineering and Physical Sciences Research Council and by the European Community Human Capital and Mobility Programme, Italian MURST and CNR (Progetto Strategico Tecnologie Chimiche Innovative).

Supporting Information Available: Derivation of eq 1 and equations employed to calculate the free energies of activation and of association, and tables listing the kinetic and thermodynamic parameters for the slipping processes (8 pages). See any current masthead page for ordering and Internet access instructions.

JA961817O

(15) Berlman, *Handbook of Fluorescence Spectra of Aromatic Compounds*, Academic Press: London, 1965.

(16) Armaroli, N.; Balzani, V.; Barigelletti, F.; De Cola, L.; Flamigni, L.; Sauvage, J.-P.; Hemmert, C. *J. Am. Chem. Soc.* **1994**, *116*, 5211−5217.